Geophys. J. Int. (2004) **156,** 701–713 doi: 10.1111/j.1365-246X.2004.02172.x

Coupled evolution of damage and porosity in poroelastic media: theory and applications to deformation of porous rocks

Y. Hamiel,[1,2] V. Lyakhovsky[2] and A. Agnon[1]

[1] *Institute of Earth Sciences, Hebrew University of Jerusalem,* 91904, *Jerusalem, Israel. E-mail: yarivh@cc.huji.ac.il*
[2] *Geological Survey of Israel,* 30 *Malkhe Israel St.,* 95501, *Jerusalem, Israel*

Accepted 2003 November 11. Received 2003 November 3; in original form 2002 September 9

SUMMARY

We address the gradual transition from brittle failure to cataclastic flow under increasing pressures by a new model, incorporating damage rheology with Biot's poroelasticity. Deformation of porous rocks is associated with growth of two classes of internal flaws, namely cracks and pores. Cracks act as stress concentrations promoting brittle failure, whereas pores dissipate stress concentrations leading to distributed deformation. The present analysis, based on thermodynamic principles, leads to a system of coupled kinetic equations for the evolution of damage along with porosity. Each kinetic equation represents competition between cracking and irreversible porosity change. In addition, the model correctly predicts the modes of strain localization such as dilating versus compacting shear bands. The model also reproduces shear dilatancy and the related change of fluid pressure under undrained conditions. For triaxial compression loading, when the evolution of porosity and damage is taken into consideration, fluid pressure first increases and then decreases, after the onset of damage. These predictions are in agreement with experimental observations on sandstones. The new development provides an internally consistent framework for simulating coupled evolution of fracturing and fluid flow in a variety of practical geological and engineering problems such as nucleation of deformation features in poroelastic media and fluid flow during the seismic cycle.

Key words: cracked media, cracks, deformation, porosity, thermodynamics.

1 INTRODUCTION

Geological evidence indicates that coupling of fluid flow and cracks in deformed porous rocks controls faulting processes and fluid flow in the earth's crust (see Hickman *et al.* 1995 for review). The evolution of fractures together with porosity is fundamental to a variety of geological problems including nucleation and growth of deformation features (Aydin & Johnson 1983; Menendez *et al.* 1996), fluid flow in fractured rocks (Renshaw 1995, 1996; Zhu & Wong 1996, 1997; Ge & Stover 2000), and the effective strength of the faulted crust and variations of pore fluid pressure during the earthquake cycle (Byerlee 1990, 1993; Rice 1992; Blanpied *et al.* 1992; Sleep & Blanpied 1992; Miller *et al.* 1996). The studies cited above have shed light on particular aspects of these geological problems and certain couplings between them. Further progress in this direction depends on our ability to incorporate various aspects of rock deformation in a unified formulation. The purpose of this paper is to develop a general framework suitable for studies of a wide variety of rock types, loading conditions and timescales.

We present a general formulation for mechanical modelling of interaction between two classes of evolving flaws: cracks and pores. We assume that the density of flaws is uniform over a length scale much larger than the length of a typical flaw, yet much smaller than the size of the entire deforming domain. For a system with a sufficiently large number of cracks and pores one can define a representative volume in which the flaw density is uniform. For such a system, one can introduce intensive variables for damage and porosity, respectively. The model combines the classic poroelastic formulation of Biot together with a distributed damage rheology model. The theoretical analysis based on thermodynamic principles leads to a system of coupled kinetic equations for the evolution of damage and inelastic porosity. The model reproduces two fundamental observations in porous rocks: the yield curve of high porosity rocks and the different modes of failure of sandstone including gradual transition from brittle failure to cataclastic flow; and the variations of fluid pressure during brittle deformation.

2 PREVIOUS WORK

In this section we review the relevant experimental work and previous modelling of yielding and damage in elastic and poroelastic rocks. Rock porosity exerts a dominant control on the style of mechanical failure. While in low-porosity crystalline rocks the yield stress increases monotonically with pressure, in high-porosity rocks there may be a yield cap at high pressure, where the slope of the yield curve has negative values for high pressure (Fig. 1). The transition from positive to negative values of the slope is related to the different modes of failure in high-porosity rocks, i.e. transition from

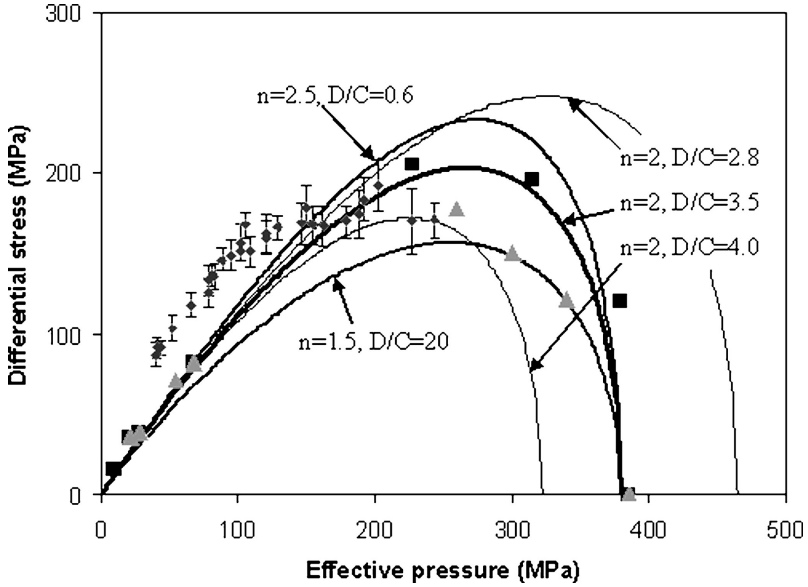

Figure 1. Experimentally measured yield stress for Berea sandstone compared with calculated curves with different values of n and of the ratio D/C (eq. 35b). Symbols indicate experimental results from Bernabe & Brace (1990) (diamonds), Wong *et al.* (1997) (squares) and Baud *et al.* (2000) (triangles). The ratio D/C is given in 10^7 MPa^{-n}. The curve corresponds to $n = 2$ and $D/C = 3.5 \cdot 10^{-7}$ MPa^{-2} provides a reasonable fit to the data from Wong *et al.* (1997).

brittle failure to cataclastic flow (Wong *et al.* 1997). Three regimes of deformation can be outlined according to the confining pressure:

(i) Failure of both low-porosity and high-porosity rocks at relatively low confining pressures is associated with dilatancy due to microcracking (Lockner *et al.* 1992; Wong *et al.* 1997). Laboratory experiments in high-porosity rocks indicate that under low effective pressure, failure is associated not only with dilatancy, but also with strain softening and the creation of localized shear dilation bands (Wong *et al.* 1997; Wong & Zhu 1999).

(ii) With the increase of effective pressure, shear bands are accompanied by strain hardening and porosity loss due to grain crushing (Menendez *et al.* 1996; Wong *et al.* 1997). Such shear bands associated with grain crushing are observed in the field (e.g. Aydin & Johnson 1978).

(iii) Failure at high effective pressure is accompanied by compaction and transition to non-localized cataclastic flow (Wong *et al.* 1997; Wong & Zhu 1999).

The analysis of deformation of fluid-saturated porous materials is based on mixture theories. Pore pressure coupled with matrix deformation was first introduced by Terzaghi (1925) with his well-known 1-D consolidation theory that relates the evolution of pore pressure to the stresses in a solid skeleton. Biot (1941) was the first to formulate a fully 3-D poroelastic theory. His now classical thermodynamic approach supplements elasticity equations for a poroelastic solid with a constitutive equation for increment of fluid content. Significant progress has been made in developing constitutive and field equations for linear poroelastic media (e.g. Nikolaevsky *et al.* 1970; Nur & Byerlee 1971; Rice & Cleary 1976). The thermodynamic approach allows construction of non-linear models for visco–elasto-plastic porous media (e.g. Biot 1973; Coussy 1995).

Fluid pressure affects rock failure and plays an important role in the seismic cycle. It reduces the frictional resistance stress via Coulomb failure criterion (Byerlee 1967), hence, this mechanism was suggested for weakening major fault zones (Byerlee 1990; Rice 1992). Fluid pressure change induced by porosity change under undrained conditions has long been recognized (see Paterson 1978 for review). Linear elasticity (Biot 1941) predicts that under undrained conditions, fluid pressure will only change proportionally to the change in the mean stress. The proportionality coefficient is known as the Skempton coefficient, B. According to Skempton (1954) the deviatoric stresses can also affect fluid pressure under undrained conditions. Following Skempton (1954) and others (Biot & Willis 1957; Hankel & Wade 1966), Lockner & Stanchits (2002) expressed the change in fluid pressure under undrained conditions, p_u, as

$$dp_u = \frac{\partial p}{\partial \sigma_m} d\sigma_m + \frac{\partial p}{\partial \tau_m} d\tau_m = B d\sigma_m + \eta\, d\tau_m, \tag{1}$$

where σ_m is the mean stress, $\tau_m = \frac{1}{2}(\sigma_1 - \sigma_3)$ is the maximal shear stress, and η is an additional coefficient that connects fluid pressure to the shear stress.

In porous rock the change in pore volume can be divided into elastic (reversible) and inelastic (irreversible) variations of the porosity. Elastic porosity variation is treated in the framework of Biot's theory of poroelasticity, and is within the order of the elastic volumetric strain. The evolution of the inelastic porosity is often treated in the framework of mechanical and chemical compaction (e.g. Rutter 1983; McKenzie 1984). Chemical compaction refers to processes such as pressure solution and mineral reaction. It is convenient to approximate the pressure-solution process by a viscous creep law (Rutter 1983; Birchwood & Turcotte 1994; Fowler & Yang 1999). In these models of pressure-solution creep or viscous compaction, the rate of porosity change is proportional to the difference between the mean stress and the fluid pressure, termed the effective pressure. The coefficient of proportionality is the inverse of the effective bulk viscosity. Models that combine the evolution of the elastic variation and inelastic variation of the porosity were suggested as more realistic descriptions of compaction in sedimentary basins (e.g. Connolly & Podladchikov 2000; Yang 2001; Suetnova & Vasseur 2000).

Several attempts have been made to extend the rate- and state-dependent friction models (e.g. Dieterich 1979, 1981; Ruina 1983) to account for fluid-fracture interaction. Sleep (1995) and Segall & Rice (1995) proposed models that combine rate- and state-dependent

friction together with porosity evolution. These models provide a framework that can be used to simulate most important aspects of the earthquake cycle. However, rate- and state-dependent friction formulation assumes that deformation is localized on pre-existing well-defined frictional surfaces. Moreover, this formulation does not provide a mechanism for understanding distributed deformation and fault nucleation.

Yielding of porous rocks, that includes brittle behaviour at low pressures and semi-brittle to cataclastic flow at high pressures, is often modelled by an elastoplastic formulation (Aydin & Johnson 1983; Olsson 1999; Issen & Rudnicki 2000; Besuelle 2001). However, this formulation does not account for fracture evolution, and uses two independent yield surfaces: shear yield surface to describe failure at the brittle region; and compactive yield surface for the semi-brittle and cataclastic flow region.

A rheological model of faulting processes in porous rocks should include the following aspects: subcritical crack growth from very early stages of the loading; material degradation due to increasing crack concentration coupled with the evolution of the inelastic porosity (dilation and compaction); gradual transition from macroscopic brittle failure to cataclastic flow; and post failure deformation and healing. The interaction and evolution of microcracks in low porosity materials have been treated in the framework of damage rheology models. Among them are Robinson's (1952) linear cumulative creep damage law, Hoff's (1953) ductile creep rupture theory, Kachanov's (1958, 1986) brittle rupture theory, Rabotnov's (1969, 1988) coupled damage creep theory, and many modifications of these theories. Several researchers (see the review of Kachanov 1994) proposed models with a scalar damage variable that fit existing experimental results reasonably well. In the study of Hansen & Schreyer (1994), the scalar isotropic damage model correlates with all measured quantities except the change in the apparent Poisson ratio. For this reason, Ju (1990) and Hansen & Schreyer (1994) suggested upgrading the damage variable from a scalar to a tensor quantity. Such an anisotropic tensorial damage model contains at least three adjustable parameters that can be used to simulate the evolution of the apparent Poisson ratio. Shao (1998) and Bart *et al.* (2000) proposed an anisotropic poroelastic damage model for saturated brittle porous materials to describe the main features related to the damage induced by microcracks, namely deterioration of poroelastic properties, evolved anisotropy and dilatancy. However, this model does not consider effects of compaction and possible microcrack closure under compressive stresses. Therefore a new model that accounts for these effects is required for describing the transition from brittle failure to cataclastic flow.

Variations of elastic moduli and Poisson's ratio with damage intensity, under different types of load, can also be described using a non-linear elastic model with scalar damage, provided that it is scaled properly with the ratio of strain invariants. This has been done in the damage model proposed by Lyakhovsky & Myasnikov (1985), Agnon & Lyakhovsky (1995) and Lyakhovsky *et al.* (1997a,b). Here we further develop that model, combining it with the classical poroelastic formulation of Biot. We use thermodynamic principles to construct a phenomenological model for coupled evolution of damage and porosity, and constrain the final model parameters by comparing the theoretical predictions with various laboratory results.

3 THERMODYNAMICS AND CONSTITUTIVE RELATIONS

We consider the porosity and damage intensity as thermodynamic state variables. The state of the system of a damageable poroelastic medium with a diffusing pore fluid is completely defined by five independent state variables: temperature, T; Cauchy elastic strain tensor, ε_{ij}; volume fluid content, ζ; inelastic porosity, ϕ; and non-dimensional damage state variable, α. Inelastic porosity refers to inelastic change in the pore volume (Coussy 1995), and it is the volume fraction of pores after complete unloading. α ranges between 0 and 1, where in undamaged material $\alpha = 0$, and failure occurs in a critical α. Although α is defined as a damage variable, it is actually responsible for the change in material stiffness: α is controlled by chemical and mechanical processes such as cracking, mechanical and chemical healing, crack sealing, pressure solution, etc.

We approach the model with irreversible thermodynamics, which provides constraints on the rates of dissipative processes (Onsager 1931; Prigogine 1955; deGroot & Mazur 1962). This approach was successfully applied to kinetics of chemical reactions and phase transitions (e.g. Fitts 1962; deGroot & Mazur 1962) and as a basis for variational methods of continuous media models (e.g. Sedov 1968; Malvern 1969). A similar approach was used as the basis for damage models (e.g. Lyakhovsky & Myasnikov 1985; Valanis 1990; Hansen & Schreyer 1994; Bart *et al.* 2000; Bercovici *et al.* 2001).

3.1 General thermodynamic relations

Following Biot's theory of poroelasticity (Biot 1941) and damage rheology (e.g. Lyakhovsky *et al.* 1997a), the free energy of a unit volume of a poroelastic solid, F, is a function of its state variables:

$$F = F(T, \varepsilon_{ij}, \zeta, \phi, \alpha). \tag{2}$$

Although we discuss below only the isothermal case, the temperature should be tracked as a state variable for the complete thermodynamic formulation. Since each variable can vary independently of the other variables, Gibbs relation can be written as (Gibbs 1961)

$$dF = -SdT + \frac{\partial F}{\partial \varepsilon_{ij}} d\varepsilon_{ij} + \frac{\partial F}{\partial \zeta} d\zeta + \frac{\partial F}{\partial \phi} d\phi + \frac{\partial F}{\partial \alpha} d\alpha, \tag{3}$$

where $S = -\frac{\partial F}{\partial T}$ is entropy density (Einstein's summation convention is assumed). The elastic strain tensor ε_{ij} is written as the difference between a total strain tensor, $\varepsilon_{ij}^{\text{tot}}$ and a strain tensor describing the inelastic deformation, $\varepsilon_{ij}^{\text{in}}$:

$$\varepsilon_{ij} = \varepsilon_{ij}^{\text{tot}} - \varepsilon_{ij}^{\text{in}}. \tag{4}$$

The equation for mass conservation of the fluid can be expressed as

$$\frac{d\zeta}{dt} + \nabla_i(q_i) = 0, \tag{5}$$

where q_i is the fluid flux with respect to the solid matrix.

The balance equations for the densities of the internal energy, U, and entropy, S, have the form (e.g. Malvern 1969; Coussy 1995):

$$\frac{dU}{dt} = \frac{d}{dt}(F + TS) = -\rho_f \nabla_i(q_i \cdot h_f) + \sigma_{ij} e_{ij} - \nabla_i Q_i, \tag{6}$$

$$\frac{dS}{dt} = -\rho_f \nabla_i(q_i \cdot s_f) - \nabla_i \left(\frac{Q_i}{T}\right) + \frac{\Phi}{T}, \Phi \geq 0, \tag{7}$$

where h_f is the enthalpy of unit mass of the fluid, which is a function of the fluid entropy of unit mass, s_f, and of the fluid pressure, ($dh_f = Tds_f + dp/\rho_f$). ρ_f is the fluid density, σ_{ij} is the stress tensor, Q_i is the heat flux, Φ is the local entropy production and the strain rate tensor e_{ij} is a temporal derivative of the total strain tensor

$$e_{ij} = \frac{d\varepsilon_{ij}^{\text{tot}}}{dt}. \tag{8}$$

The balance eqs (6) and (7) differ from the similar energy and entropy balance equations for elastic media with distributed damage (Lyakhovsky *et al.* 1997a) by the divergence term related to the energy and entropy advection due to pore fluid transport.

The stress tensor and the fluid pressure are defined as (Malvern 1969; Coussy 1995):

$$\sigma_{ij} = \frac{\partial F}{\partial \varepsilon_{ij}}, \tag{9}$$

$$p = \frac{\partial F}{\partial \zeta}, \tag{10}$$

where, it should be emphasized, the inelastic porosity is kept constant in these derivatives. Substituting Gibbs relation (3) into the energy and entropy balance eqs (6) and (7), using the fluid conservation eq. (5) and the definitions of the stress tensor and the fluid pressure (9, 10), the local entropy production may be represented as

$$\Phi = -\frac{Q_i}{T}\nabla_i T + \sigma_{ij}\frac{d\varepsilon_{ij}^{\text{in}}}{dt} - q_i \nabla_i p - \frac{\partial F}{\partial \alpha}\frac{d\alpha}{dt} - \frac{\partial F}{\partial \phi}\frac{d\phi}{dt} \geq 0. \tag{11}$$

Each term in this equation represents entropy production due to a different physical process and can be classified according to its tensorial rank. Thus in eq. (11): the first term describes entropy production by heat conduction; the second term is due to viscous dissipation; the third term is related to the fluid transport process; and the last two terms are respectively related to internal energy changes caused by mirocracking and inelastic porosity change. As a standard approach, we split terms of different tensorial rank. Therefore, the viscous dissipation term is divided into volumetric and deviatoric parts. This separation is consistent with the distinction between shear and bulk viscosities (McKenzie 1984). We now introduce the notation τ_{ij} and $\tilde{\varepsilon}_{ij}$ for the deviatoric stress and strain tensors, and ε_{kk} and $\sigma_m (\sigma_m = -\frac{1}{3}\sigma_{kk})$ for the volumetric strain and mean stress. Using this notation, eq. (11) can be rewritten as

$$\Phi = -\frac{Q_i}{T}\nabla_i T + \tau_{ij}\frac{d\tilde{\varepsilon}_{ij}^{\text{in}}}{dt} - \sigma_m \frac{d\varepsilon_{kk}^{\text{in}}}{dt} - q_i \nabla_i p - \frac{\partial F}{\partial \alpha}\frac{d\alpha}{dt} - \frac{\partial F}{\partial \phi}\frac{d\phi}{dt} \geq 0. \tag{12}$$

Each term in eq. (12) may be viewed as a product of a thermodynamic flux and a thermodynamic force (deGroot & Mazur 1962; Malvern 1969). For example, in the first term the thermodynamic force is the temperature gradient and the thermodynamic flux is the heat flux.

To complete the formulation we now have to write constitutive equations relating the thermodynamic fluxes to the thermodynamic forces. Usually the components of the various fluxes do not depend on all the forces. According to Curie's theorem, in an isotropic medium, fluxes and forces of different tensorial rank cannot be coupled (e.g. deGroot & Mazur 1962). Hence, scalar, vectorial and tensorial terms in eq. (12) represent dissipation processes of different physical natures and, accordingly, should be non-negative independently of the others. The condition of non-negative local entropy production when divided into three independent conditions becomes:

$$\Phi_{\text{scalar}} = -\frac{\partial F}{\partial \alpha}\frac{d\alpha}{dt} - \frac{\partial F}{\partial \phi}\frac{d\phi}{dt} - \sigma_m \frac{d\varepsilon_{kk}^{\text{in}}}{dt} \geq 0, \tag{13}$$

$$\Phi_{\text{vector}} = -\frac{Q_i}{T}\nabla_i T - \frac{1}{\rho_f} q_i \nabla_i p \geq 0, \tag{14}$$

$$\Phi_{\text{tensor}} = \tau_{ij}\frac{d\tilde{\varepsilon}_{ij}^{\text{in}}}{dt} \geq 0. \tag{15}$$

A usual assumption of a plastically incompressible matrix means that an irreversible change in the bulk volume is equal to an inelastic porosity change. Thus, the time derivative of the trace of the inelastic strain tensor, $\varepsilon_{kk}^{\text{in}}$, is equal to time derivative of the inelastic porosity, and Φ_{scalar} can be rewritten as

$$\Phi_{\text{scalar}} = -\frac{\partial F}{\partial \alpha}\frac{d\alpha}{dt} - \left(\frac{\partial F}{\partial \phi} + \sigma_m\right)\frac{d\phi}{dt} \geq 0. \tag{16}$$

For sufficiently small deviations from equilibrium, a constitutive equation gives the thermodynamic flux as a linear function of the thermodynamic force for each dissipation (deGroot & Mazur 1962; Malvern 1969; Bear 1972). These phenomenological equations guarantee the non-negative value of entropy production. Non-negativity of Φ_{vector} gives rise to Fourier's law (17) for the thermal conduction and Darcy's law (18) for the fluid transport:

$$Q_i = -\chi \cdot \nabla_i T, \tag{17}$$

$$q_i = -\kappa \cdot \nabla_i p, \tag{18}$$

where χ and κ are the thermal and hydraulic conductivities, respectively. Non-negativity of Φ_{tensor} gives rise to Newton's relation for viscous flow

$$\tau_{ij} = 2\eta_s \frac{d\tilde{\varepsilon}_{ij}^{\text{in}}}{dt}, \tag{19}$$

where η_s is the shear viscosity. Similarly, to assure non-negativity of Φ_{scalar}, we write the phenomenological equations for the kinetics of the internal state variables α and ϕ as a set of two coupled differential equations:

$$\begin{aligned} \frac{d\phi}{dt} &= C_{\phi\phi}\left(\frac{\partial F}{\partial \phi} + \sigma_m\right) + C_{\phi\alpha}\frac{\partial F}{\partial \alpha}, \\ \frac{d\alpha}{dt} &= C_{\alpha\phi}\left(\frac{\partial F}{\partial \phi} + \sigma_m\right) + C_{\alpha\alpha}\frac{\partial F}{\partial \alpha}, \end{aligned} \tag{20}$$

where the matrix of the kinetic coefficients, C, has to satisfy the following conditions (deGroot & Mazur 1962; Bear 1972):

$$C_{\phi\phi} \leq 0, \quad C_{\alpha\alpha} \leq 0, \quad 4 \cdot C_{\phi\phi} C_{\alpha\alpha} \geq (C_{\phi\alpha} + C_{\alpha\phi})^2. \tag{21}$$

Owning to Onsager's reciprocal relations the matrix of the kinetic coefficients C is usually taken to be either symmetric or antisymmetric (Malvern 1969). The kinetic eqs (20) describe the change in inelastic porosity and, respectively, in terms of derivatives of the free energy. For full understanding of the kinetic equations and estimation of the kinetic coefficients, C, we have to express the free energy as a function of its state variables.

3.2 Equations of state

Following Biot's (1941, 1956) formulation, the isothermal free energy for linear poroelastic media, F, is represented as a sum of the elastic energy under drained conditions and the poroelastic coupling term of the saturated medium:

$$F = F_{dr}(\varepsilon_{ij}, \alpha, \phi) + \frac{1}{2} M \cdot [\beta I_1 - (\zeta - \phi)]^2, \tag{22}$$

where M and β are the Biot's modulus and coefficient for porous media and $I_1 = \varepsilon_{kk}$ is the first invariant of the elastic strain tensor. Following Lyakhovsky *et al.* (1997a), who wrote the elastic energy, F_{dr}, for non-linear damaged media, the elastic energy under drained conditions is written as:

$$F_{dr} = \frac{\lambda}{2} I_1^2 + \mu I_2 - \gamma I_1 \sqrt{I_2}, \tag{23}$$

where $I_2 = \varepsilon_{ij}\varepsilon_{ij}$ is the second invariant of the elastic strain tensor; λ and μ are the Lame drained moduli; and, γ is the strain coupling modulus which accounts for the material non-linearity (Lyakhovsky *et al.* 1997a). Substituting the free energy (22, 23) into the equations of state (9, 10), we obtain constitutive relations for the stresses and fluid pressure under isothermal conditions:

$$\sigma_{ij} = \left(\lambda - \frac{\gamma}{\xi}\right) I_1\delta_{ij} + (2\mu - \gamma\xi)\varepsilon_{ij} + \beta M[\beta I_1 - (\zeta - \phi)]\delta_{ij}, \quad (24)$$

$$p = M[-\beta I_1 + (\zeta - \phi)], \quad (25)$$

where ξ is the strain invariant ratio $I_1/\sqrt{I_2}$. For all deformations $-\sqrt{3} \le \xi \le \sqrt{3}$, where for isotropic compaction $\xi = -\sqrt{3}$, for isotropic dilation $\xi = \sqrt{3}$, and for isochoric shear $\xi = 0$. Eq. (24) for the total stress may be rewritten in terms of effective stress and fluid pressure

$$\sigma_{ij} = \sigma^e_{ij} - \beta p\delta_{ij}, \quad (26)$$

where the effective stress is:

$$\sigma^e_{ij} = \left(\lambda - \frac{\gamma}{\xi}\right) I_1\delta_{ij} + (2\mu - \gamma\xi)\varepsilon_{ij}. \quad (27)$$

In the present generalization of Biot's formulation and Lyakhovsky's model, the elastic moduli λ, μ and γ are assumed to depend on the damage variable α and inelastic porosity ϕ. Agnon & Lyakhovsky (1995) analysed the connection between the elastic moduli and α. They assumed constant λ and the following linear approximations: $\mu = \mu_0 + \mu_1\alpha$, $\gamma = \gamma_1\alpha$, with μ_0, μ_1 and γ_1 constants for each material. The existence of critical strain invariant ratio ξ_0 (Agnon & Lyakhovsky 1995), which corresponds to a neutral state between weakening (growth in α) and hardening (reduction in α) of the medium, reduces the relation for μ to $\mu = \mu_0 + \gamma_1\xi_0\alpha$. ξ_0 was related to the friction angle and it was found to be negative on the order of unity from a variety of experimental measurements (Lyakhovsky *et al.* 1997a; Liu *et al.* 2001). Here, we adopt these relations between elastic moduli and the damage variable α to account for the effect of microcrack concentration on the elastic properties of the bulk. We also assume that microcracks do not directly change the fluid energy. Hence, Biot modulus, M, and Biot coefficient, β, do not depend on α. On the other hand, the poroelastic moduli decrease with increase in porosity (e.g. Dvorkin *et al.* 1994; Mavko & Mukerji 1995). Viewing the porosity as a concentration of roughly spherical inclusions, the elastic properties of the bulk linearly decrease with increasing ϕ (e.g. Christensen 1979). This linear relation is the first order approximation to more general models for the effective moduli and their dependence on porosity in poroelastic media (e.g. Dvorkin *et al.* 1994; Mavko & Mukerji 1995; Hudson 2000). This linear approximation is supported by experiments on sandstone reported by Dvorkin & Nur (1996). Hence, the elastic moduli are assumed to be proportional to the term $(1 - \phi/\phi_{cr})$, where ϕ_{cr} is the porosity upper bound in which the material loses its stiffness. Finally, the effective poroelastic moduli can be written as:

$$\lambda = \lambda_0\left(1 - \frac{\phi}{\phi_{cr}}\right), M = M_0\left(1 - \frac{\phi}{\phi_{cr}}\right),$$
$$\mu = \left(1 - \frac{\phi}{\phi_{cr}}\right)(\mu_0 + \xi_0\gamma_1\alpha), \gamma = \left(1 - \frac{\phi}{\phi_{cr}}\right)\gamma_1\alpha. \quad (28)$$

In the following, we have adopted Terzaghi's assumption ($\beta = 1$) as a useful approximation (see discussion in Nur & Byerlee 1971). The effective stress then becomes the sum of the total stress and the fluid pressure. Eqs (24)–(27) reduce to the equations of state developed by Biot (1941, 1956) for linear poroelastic media in the limit of zero damage intensity ($\alpha = 0$. At the same time these equations reduce to the stress-strain relations derived by Lyakhovsky *et al.* (1997a) for damaged elastic media with vanishing fluid pressure ($p = 0$).

4 KINETICS OF DAMAGE AND INELASTIC POROSITY

The kinetics of damage and inelastic porosity are functions of the thermodynamic forces $\partial F/\partial\alpha$ and $\partial F/\partial\phi$, andg (eq. 20). Using eqs (22), (23) and the constitutive equations for the elastic moduli (28), $\partial F/\partial\alpha$ and $\partial F/\partial\phi$ can be written as:

$$\frac{\partial F}{\partial\phi} = -p + O(\varepsilon^2),$$
$$\frac{\partial F}{\partial\alpha} = -\left(1 - \frac{\phi}{\phi_{cr}}\right)\gamma_1 I_2(\xi - \xi_0). \quad (29)$$

Substituting (29) into (20) and the neglecting high order terms in $\partial F/\partial\phi$, the kinetic equations become:

$$\frac{d\phi}{dt} = C_{\phi\phi}P_e + C_{\phi\alpha}\left[-\left(1 - \frac{\phi}{\phi_{cr}}\right)\gamma_1 I_2(\xi - \xi_0)\right], \quad (30a)$$

$$\frac{d\alpha}{dt} = C_{\alpha\phi}P_e + C_{\alpha\alpha}\left[-\left(1 - \frac{\phi}{\phi_{cr}}\right)\gamma_1 I_2(\xi - \xi_0)\right], \quad (30b)$$

where the effective pressure $P_e = -\frac{1}{3}\sigma^e_{kk}$. For applications of the kinetic eqs (30a) and (30b) we seek estimates for the kinetic coefficients matrix, C_{ij}, in the following subsection.

4.1 Constraints on kinetic coefficients

Useful constraints can be put on the diagonal terms of the kinetic coefficient matrix ($C_{\phi\phi}$, $C_{\alpha\alpha}$). Lyakhovsky *et al.* (1997a) analysed damage evolution in crystalline and high-porosity rocks, and found $C_{\alpha\alpha}$ to be between $-0.5/\gamma_1$ and $-10/\gamma_1$ 1/(Pa s) for unsaturated rocks. The rate of fracture process in saturated rocks differs from that in unsaturated rocks, but not in order of magnitude (Dennis & Atkinson 1982; Masuda 2001). Therefore, $C_{\alpha\alpha}$ in our model is of the same order of magnitude of $C_{\alpha\alpha}$ found by Lyakhovsky *et al.* (1997a). $C_{\phi\phi}$ is the inverse of the bulk viscosity in viscous compaction models (McKenzie 1984; Fowler 1990), and is estimated to be in the order of 10^{-18}–10^{-22} 1/(Pa s) for sedimentary basins (Suetnova & Vasseur 2000; Yang 2001). In these models and models of pressure solution creep (Lahner 1995; Paterson 1995; Fowler & Yang 1999) $C_{\phi\phi}$ is usually given as a power-law of the porosity ($C_{\phi\phi} = A\phi^m$), where the exponent, m, ranges between one and three for most rocks (Paterson 1995) and A in the order of 10^{-16}–10^{-22} 1/(Pa s).

Constraints on the coupling terms ($C_{\phi\alpha}$, $C_{\alpha\phi}$) are less known. We consider the behaviour of sandstones as a guide to constraining $C_{\phi\alpha}$ and $C_{\alpha\phi}$. Triaxial compression experiments of sandstones (Zhang *et al.* 1990; Wong *et al.* 1997) have shown that acoustic emission, or damage increase, related to grain crushing occurs at relatively high effective pressure. Since the second term in damage kinetic eq. (30b) is negative under high pressures, corresponding to material recovery (healing), this observation of grain crushing demands positive $C_{\alpha\phi}$. At the same time, grain crushing leads to significant reduction of the inelastic porosity, corresponding to a negative value of $C_{\phi\alpha}$. This entails that the matrix of kinetic coefficients be antisymmetric

(Malvern 1969), and conditions (21) reduce to

$$C_{\phi\phi} \leq 0, \quad C_{\alpha\alpha} \leq 0, \quad C_{\phi\alpha} = -C_{\alpha\phi}. \tag{31}$$

Grain crushing was observed in isotropic pressing experiments only in high-porosity rocks under high effective pressures (Zhang *et al.* 1990). The first term in the damage evolution eq. (30b) should overcome the negative value of the second term at high effective pressures and high porosities. Under isotropic pressing the rate of the second term in (30b) is proportional to the square of the effective pressure. Hence, we choose $C_{\alpha\phi}$ to be a power-law of the porosity and effective pressure ($C_{\alpha\phi} = D\phi^{\tilde{n}} P_e^n$), and this leads to a rate of damage increase proportional to $P_e^{(n+1)}$ with n greater than unity. Various power laws in the effective pressure are frequently encountered in related formulations of granular mechanics (e.g. Biot 1973) and dislocation creep (e.g. Poirier 1985). Eq. (30b) describes competition between two terms; the first term is dominant at high pressures and the second term is dominant under relatively low pressures. The competition between damage increase due to stress concentration at the grain contacts (first term in (30b) and damage decrease due to healing (second term in 30b) enables definition of a critical effective pressure, $P_e^{\rm cr}$, from the condition:

$$D\phi^{\tilde{n}} \left(P_e^{\rm cr}\right)^{n+1} + C_{\alpha\alpha}\left[\left(1 - \frac{\phi}{\phi_{\rm cr}}\right)\gamma_1 I_2\left(\sqrt{3} + \xi_0\right)\right] = 0. \tag{32}$$

This pressure corresponds to the onset of damage for isotropic pressing. For $\phi\ /\phi_{\rm cr} \ll 1$ and $I_2 = (P_e^{\rm cr}/K)^2$ (K is the bulk modulus) eq. (32) leads to an expression for the critical effective pressure:

$$P_e^{\rm cr} \approx \left(\frac{-C_{\alpha\alpha}\gamma_1\left(\sqrt{3} + \xi_0\right)}{K^2 D\phi^{\tilde{n}}}\right)^{\frac{1}{n-1}} \tag{33}$$

or, for experimentally determined critical effective pressure, to the estimation of the kinetic coefficient, D:

$$D \approx \frac{-C_{\alpha\alpha}\gamma_1\left(\sqrt{3} + \xi_0\right)}{K^2\phi^{\tilde{n}}}\left(P_e^{\rm cr}\right)^{1-n}. \tag{34}$$

Theoretical formulation based on the Hertzian contact theory (Zhang *et al.* 1990) predicts that the critical effective pressure for a given grain size increases proportionally to the power of the porosity, i.e. $P_e^{\rm cr} \propto \phi^{-3/2}$. Experimental data of the critical pressure in various sandstones (Zhang *et al.* 1990; Wong *et al.* 1997) show reasonable agreement with this theoretical prediction. By inspection of the power dependence predicted by the Hertzian contact theory versus eq. (33), we note that $\tilde{n} = \frac{3}{2}(n-1)$. Finally, taking into account all these conditions, the kinetic eqs (30a) and (30b) can be rewritten as

$$\frac{d\phi}{dt} = -A\phi^m P_e + D\left(1 - \frac{\phi}{\phi_{\rm cr}}\right)\phi^{3(n-1)/2} P_e^n \gamma_1 I_2(\xi - \xi_0), \tag{35a}$$

$$\frac{d\alpha}{dt} = D\phi^{3(n-1)/2} P_e^{n+1} + C\left(1 - \frac{\phi}{\phi_{\rm cr}}\right)\gamma_1 I_2(\xi - \xi_0), \tag{35b}$$

where m ranges between one and three. A is in the order of 10^{-16}–10^{-22} 1/(Pa s) depending on the power m, and therefore is negligibly small for laboratory timescale. C is in the order of $0.5/\gamma_1$ to $10/\gamma_1$ 1/(Pa s). D and n will be constrained in the next subsection from the analysis of the yield curve of sandstones.

4.2 Yielding of porous rocks

We associate yielding (termed first yielding occasionally) with the onset of damage. The stress-strain relation becomes non-linear when the modulus γ is greater then zero (eq. 24). Since γ is proportional to the damage variable α, the stress-strain relation becomes nonlinear upon the onset of damage. The calculated yield curve for damageable poroelastic rock, defined as the locus of onset of damage, is shown in Fig. 1. The shape of the curve is determined by the competition between the first and second terms in the equation for damage evolution (35b). For low effective pressures the second term is dominant, causing a positive slope of the curve, whereas for high effective pressures the first term becomes dominant, causing a negative slope. The transition from positive to negative values of the slope is determined by the ratio of constants, D/C, and the power, n, in eq. (35b). Increase of the ratio, D/C, causes the yield cap (negative values of the slope) to appear at lower effective pressure, whereas the increase of n results in a steeper yield cap.

The ratio D/C and the power n can be estimated by comparing the theoretical yield stress with experimentally observed data. The measured values of yield stress for Berea sandstone samples (markers in Fig. 1) from Bernabe & Brace (1990), Wong *et al.* (1997) and Baud *et al.* (2000) show significant scattering between data sets reported by different authors. Thus, the calculated yield curve can fit only one of the presented data sets. Fig. 1 demonstrates considerable agreement between the measured values of yield stress for Berea sandstone samples reported by Wong *et al.* (1997) and the theoretical curve for $D/C = 3.5 \times 10^{-7}$ (MPa)$^{-n}$ and $n = 2$. Liu *et al.* (2001) and Hamiel *et al.* (2004) estimated that $C = 3.2 \times 10^{-4}$ MPa^{-1} s^{-1} for Berea sandstone. This value and our estimation for the ratio D/C, gives a value of $D = 1.1 \times 10^{-10}$ MPa^{-3} s^{-1} for Berea sandstone. In these calculations we also used the values $\lambda_0 = 8.8 \times 10^9$ Pa, $\mu_0 = 1.5 \times 10^{10}$ Pa, $\xi_0 = -1.19$ estimated by Liu *et al.* (2001) and Hamiel *et al.* (in prep.) for Berea sandstone, and inelastic porosity $\phi = 0.2$. These values were also used for the simulations presented in the next section (Figs 3, 6 and 7).

5 MODEL APPLICATIONS

5.1 Modes of deformation: from brittle failure to cataclastic flow

Previous damage rheology models (e.g. Lyakhovsky *et al.* 1997a) account for material weakening under high deviatoric stresses relative to confining pressures, and healing at high pressures and low deviatoric stresses. Agnon & Lyakhovsky (1995) introduced a critical strain invariant ratio, ξ_0, corresponding to the transition from material weakening to healing, and related its value to the friction angle of low-porosity rocks. Lyakhovsky *et al.* (1997a) show that the second term in the equation for damage evolution (35b) contributes to localization of the damage for $\xi > \xi_0$. Fig. 2(a) shows schematically the yield stress or onset of damage for brittle rock only (Lyakhovsky *et al.* 1997a), defined by the curve $\xi = \xi_0$. Fig. 2(a) also shows the field of degradation ($d\alpha/dt > 0$) and the field of healing ($d\alpha/dt < 0$). Here, the presence of inelastic porosity and the competition between the first and the second terms in (35b) shifts the transition from material weakening to healing of the critical strain invariant ratio to lower values. Now material weakening starts at $\xi = \xi^*$ defined by:

$$\xi^* = \xi_0 - \frac{D\phi^{3(n-1)/2} P_e^{n+1}}{C(1 - \phi/\phi_{\rm cr})\gamma_1 I_2}. \tag{36}$$

The curve $\xi = \xi^*$ that is consistent with the yield curve in our model is shown schematically in Fig. 2(b) (heavy line). Since A (35a) is usually negligibly small for laboratory timescale, the transition from inelastic compaction ($d\phi/dt < 0$) to inelastic dilation ($d\phi/dt > 0$)

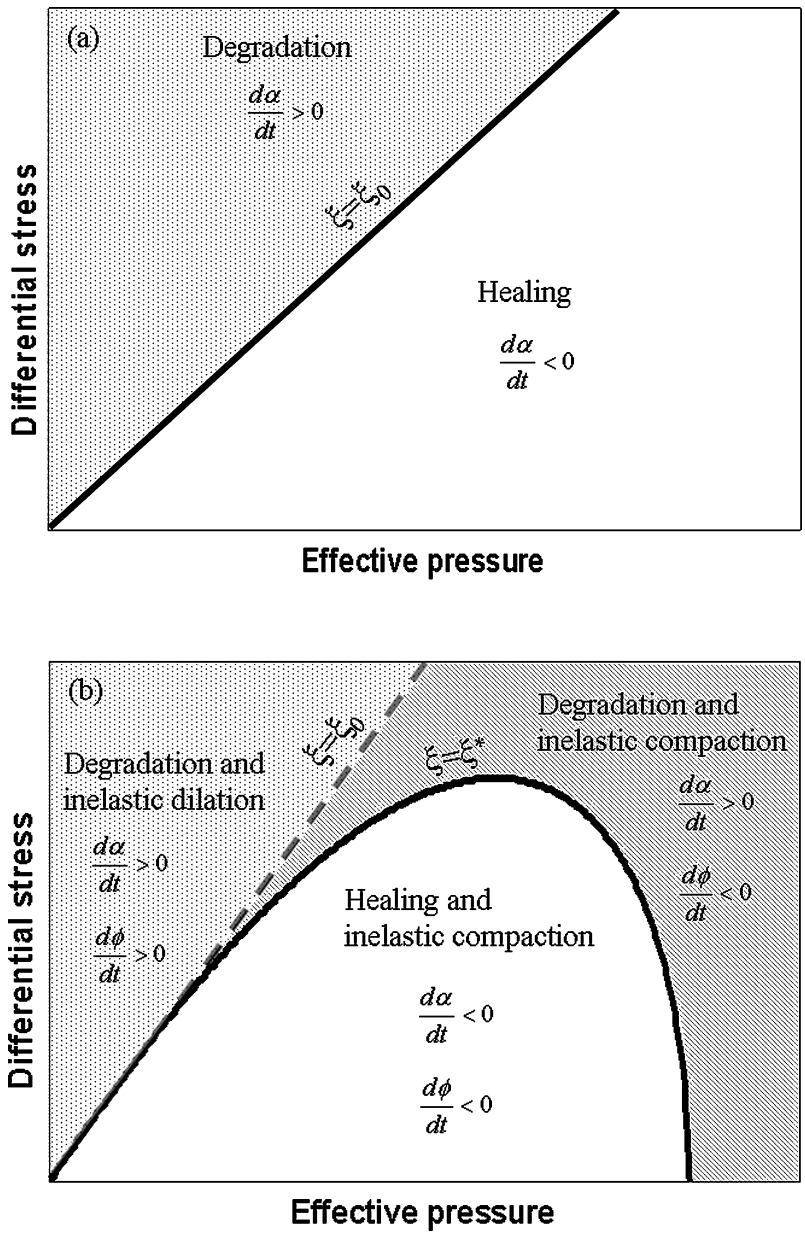

Figure 2. (a) Schematic yield curve of low-porosity brittle rocks. The curves denote the onset of damage at $\xi = \xi_0$ (Lyakhovsky *et al.* 1997a). Degradation ($d\alpha/dt > 0$) occurs whenever $\xi > \xi_0$ and healing ($d\alpha/dt < 0$) when $\xi < \xi_0$. (b) Schematic yield curve ($\xi = \xi^*$) and stability fields of high-porosity rocks in the present model. Three stability fields in respect to damage and inelastic porosity evolution are shown: degradation and inelastic dilation (dotted area); degradation and inelastic compaction (stippled area); and, healing and inelastic compaction. See Fig. 1 for some experimental data.

occurs at $\xi = \xi_0$ (35a). Fig. 2(b) shows three stability fields in respect of damage and inelastic porosity evolution: degradation and inelastic dilation at relatively low effective pressures and high differential stresses; degradation and inelastic compaction at relatively high effective pressures; and healing and inelastic compaction at relatively low effective pressures and low differential stresses. As we show below in this section, the transition from inelastic dilation to inelastic compaction is related to the transition from brittle failure to cataclastic flow.

The total volumetric change is determined by the sum of the elastic and inelastic volumetric change. Since the matrix was assumed to be plastically incompressible, the total volumetric change, $\delta V/V$, can be written as

$$\frac{\delta V}{V} = I_1 + \delta\phi. \tag{37}$$

where $\delta\phi$ is the change in the inelastic porosity. The transition between dilation and compaction occurs when $I_1 = -\delta\phi$, or in terms of the strain invariant ratio $\xi = -\delta\phi/I_2$. Fig. 3 shows drained simulations of the differential stress versus $\delta V/V$ from initial condition of isotropic compression. Dilatancy is obtained under low confining pressure simulations (Fig. 3a) and compaction under high confining pressures (Fig. 3b). Fig. 3 also shows the plastic behaviour of the stress-strain relation under high effective pressure. The theoretical predictions in Fig. 3 are in qualitative agreement with experimental observations in sandstones (Menendez *et al.* 1996; Wong *et al.* 1997; Wong & Zhu 1999).

Triaxial compression tests on sandstones (Menendez *et al.* 1996; Wong *et al.* 1997) show three main modes of deformation: cataclastic flow at high effective pressures; compacting shear bands at lower effective pressures; and dilating shear bands at lowest effective

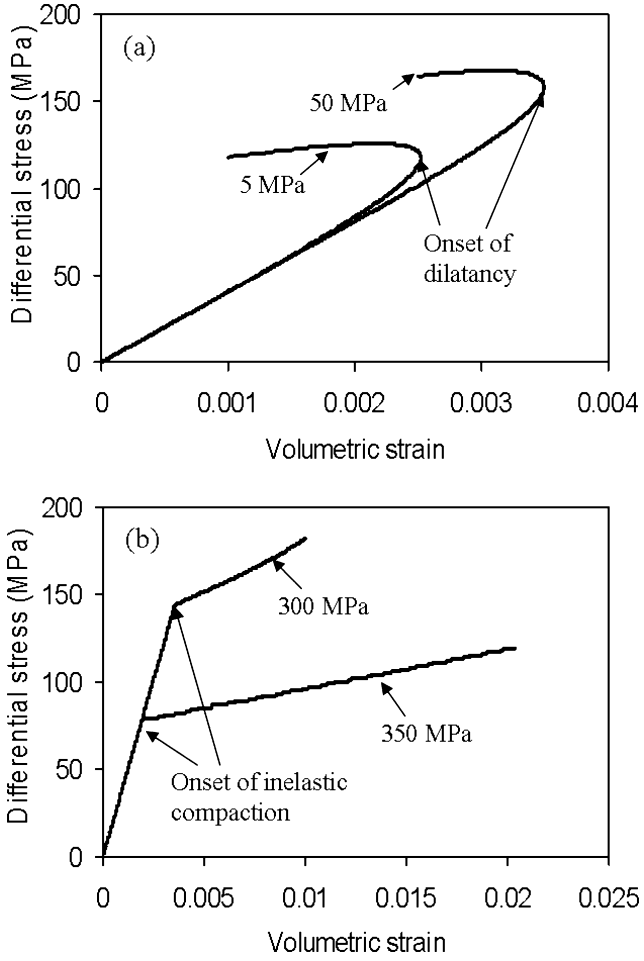

Figure 3. Calculated curves of differential stress versus total volumetric strain change, with initial conditions of isotropic pressing, under triaxial compression simulations. (a) Curves at relatively low effective confining pressure ($\sigma_{22}^{ef} = \sigma_{33}^{ef} = 5$, 50 MPa), showing dilatancy. (b) Curves at relatively high effective confining pressure (300, 350 MPa), showing shear-enhanced compaction.

pressures. Fig. 4 schematically shows three different scenarios of material evolution in (α, ξ) coordinates, corresponding to the three modes of deformation observed in laboratory experiments. All three paths in Fig. 4 start with isotropic compression ($\xi = -\sqrt{3}$), analogous to most triaxial compression experiments. Path (I) represents deformation at high effective pressures. During path (I), while increasing the differential stress, ξ exceeds ξ^* causing onset of damage. As a result of the high effective pressure ξ will not cross ξ_0, causing only non-localized damage. Damage in this path is accompanied with compaction and plastic behaviour of the stress-strain relation (Fig. 3b). Path (I) corresponds to the experimentally observed cataclastic flow (Menendez *et al.* 1996; Wong *et al.* 1997). Paths (II) and (III) represent deformation at intermediate and low effective pressures respectively. At lower effective pressures than in path (I) ξ will exceed ξ_0 before failure causing localized damage to develop (paths (II) and (III)). For relatively intermediate effective pressures the localized damage is accompanied by compaction (path (II)), corresponding to compacting shear bands (Menendez *et al.* 1996; Wong *et al.* 1997). For low effective pressures failure is preceded first by compaction followed by dilatancy (path (III) in Fig. 4, see also Fig. 3a). Path (III) corresponds to dilating shear bands observed in laboratory experiments under low effective pressures (Menendez *et al.* 1996; Wong *et al.* 1997).

5.2 Undrained poroelastic response

Our model predicts that for undrained response the fluid pressure depends on the damage intensity (α). Similarly to recent experimental results reported by Lockner & Stanchits (2002), we examine the change of fluid pressure under undrained conditions at different deviatoric stresses. We present simulations based on our model for triaxial loading ($\sigma_2 = \sigma_3$). During these simulations fluid volume content, ζ, was set constant to mimic undrained conditions. Fig. 5 shows the measured poroelastic coefficients B, η from eq. (1) for Navajo sandstone (Lockner & Stanchits 2002) compared with the calculated values for different damage intensities and different values of $\tau_m (\tau_m = \frac{1}{2}(\sigma_1 - \sigma_3))$. Fig. 5 reveals that Skempton coefficient, B, in our model is about constant or slightly increases with shear stress and damage intensity. Unlike B, $|\eta|$ strongly depends on the shear stress and on damage, increasing with both τ_m and α. Fig. 5 demonstrates quantitative agreement between the measured values of B and η for Navajo sandstone samples (Lockner & Stanchits 2002) and the values calculated for $\alpha = 0.2$. Fig. 6 shows the change in the fluid pressure, from an initial value of 10 MPa, as a function of τ_m for a given damage intensity (α). In these simulations the mean stress was kept constant ($\sigma_1 + 2\sigma_3 = \text{constant}$), thus, fluid pressure changes according to the change of η. For a given α, $|\eta|$ increases with τ_m and therefore fluid pressure decreases

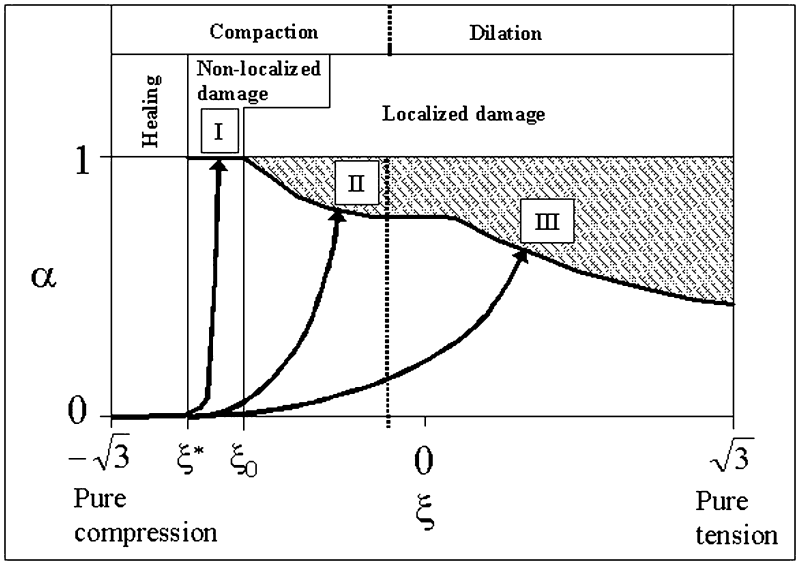

Figure 4. Stability fields and modes of deformation. Thick curve represents maximum value of damage variable (α) as a function of the strain invariant ratio ξ. The maximum value of α was calculated using conditions for loss of convexity (see also eqs 14 and 15 in Lyakhovsky *et al.* 1997a). The range $-\sqrt{3} < \xi < \xi_0$ corresponds to non-localized damage distribution, and the range $\sqrt{3} > \xi > \xi_0$ corresponds to the appearance of localized damage, where onset of damage occurs at $\xi = \xi^*(\xi^*$ varies according to eq. 36). The transition from compaction to dilation occurs between ξ_0 and $\xi = 0$, depending on the loading and material properties. Three different typical paths are illustrated: (I) deformation accompanied by compaction and non-localized damage, corresponding to cataclastic flow; (II) deformation accompanied by compaction and localized damage, corresponding to compacting shear bands; (III) deformation accompanied by dilation and localized damage, corresponding to dilating shear bands. The stippled area represented an unstable post-failure state.

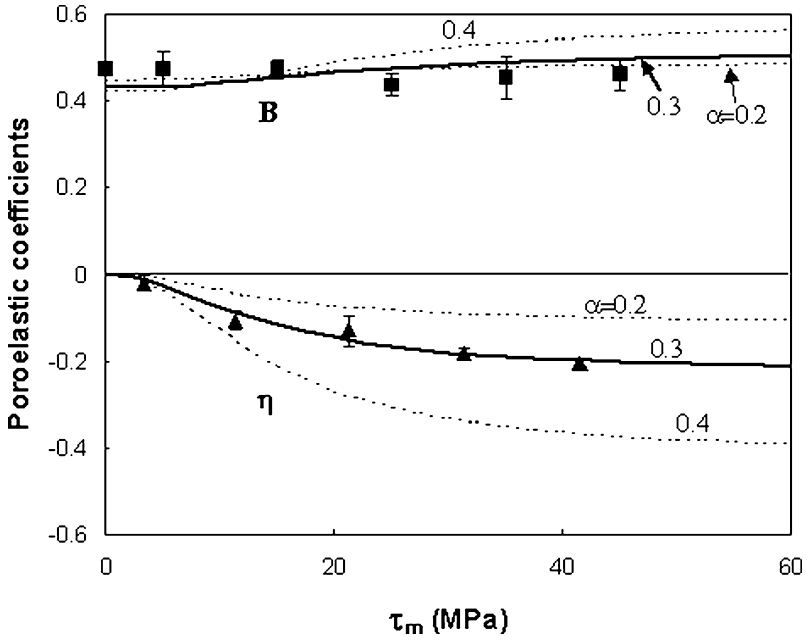

Figure 5. Measured poroelastic coefficients B, η from eq. (1) for Navajo sandstone (Lockner & Stanchits 2002) compared with the calculated values for different damage intensity and different values of $\tau_m = \frac{1}{2}(\sigma_1 - \sigma_3)$. $\alpha = 0.2$ gives quantitative agreement between the measured and the calculated values of B and η for Navajo sandstone.

concomitantly. This reduction in fluid pressure occurs mainly by dilatancy of fractures, represented by the non-linear term in the elastic energy (eq. 23, see also eq. 27). Therefore, at $\alpha = 0$ fluid pressure remains constant and the higher α, the more drastic the reduction in p.

Evolution of fluid pressure during undrained triaxial compression simulations, taking into account the kinetics of damage and porosity, is illustrated in Fig. 7. In these simulations confining pressure was kept constant ($\sigma_2 = \sigma_3 =$ constant) and σ_1 was ramped with a constant loading rate of 0.1 MPa s^{-1}, which approximately corresponds to a strain rate of 10^{-5} s^{-1} in the linear elastic region. During the simulation the fluid pressure first increases according to predictions of linear poroelasticity (Fig. 7a). Later, after onset of damage, increase in the differential stress causes a decrease in the fluid pressure. Since B does not change much with damage (Fig. 5), the decrease in the fluid pressure is mostly caused by the damage-related

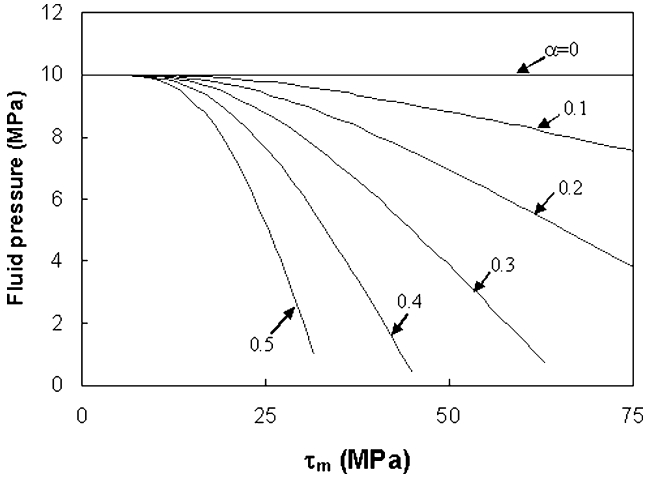

Figure 6. Calculated curves of fluid pressure verses $\tau_m = \frac{1}{2}(\sigma_1 - \sigma_3)$ at constant mean stress ($d\sigma_1 = -2d\sigma_3$) under undrained conditions. Each line represents a different value of the damage variable (α), where the line $\alpha = 0$ corresponds to linear poroelasticity. In this calculation $dp = \eta\, d\tau_m$ (after Lockner & Stanchits 2002), where p is fluid pressure. The initial value of fluid pressure is 10 MPa, and mean stress was kept at 50 MPa.

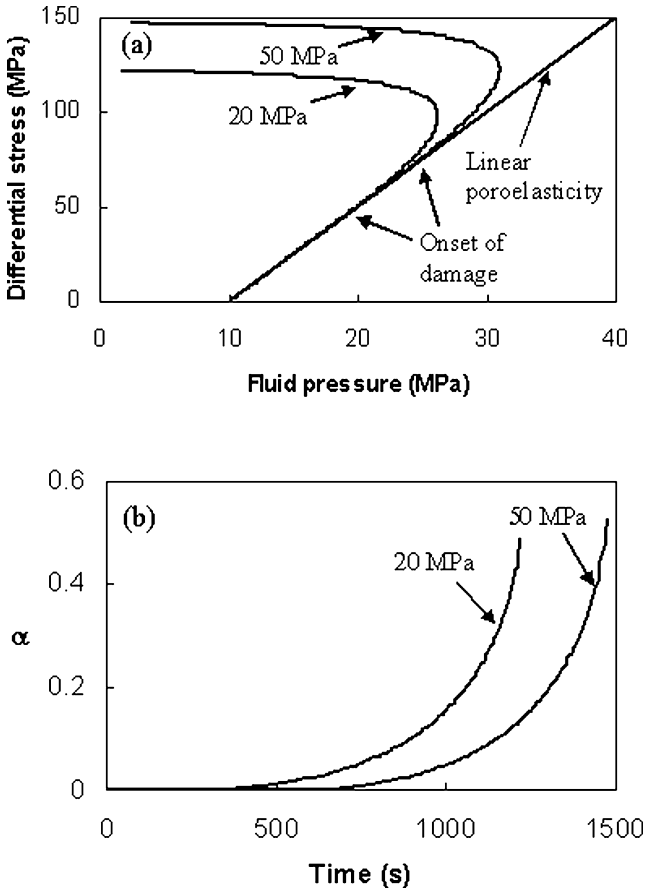

Figure 7. (a) Fluid pressure evolution, during triaxial compression simulations, under undrained conditions at a loading rate of 0.1 MPa s^{-1} for two different confining pressures (20, 50 MPa). Straight line corresponds to the evolution of fluid pressure according to linear poroelasticity. (b) Damage evolution of the two simulations in (a).

increase in $|\eta|$. This increase corresponds to dilatancy hardening in undrained triaxial tests. Similar increase and following decrease of fluid pressure during triaxial compression tests under undrained conditions was observed in laboratory experiments on porous rocks (e.g. Paterson 1978).

6 DISCUSSION

We have presented here a model for coupled evolution of damage and porosity in poroelastic media, based on thermodynamic principles and experimental observations. The model indicates the importance

of the interaction between damage and fluid flow. Our formulation combines the classical poroelasticity model of Biot (1941) together with the damage rheology of Lyakhovsky *et al.* (1997a). Our combined model provides a framework to explore kinetic processes in poroelastic rocks and can be applied to a variety of geological problems concerning damage evolution and fluid flow.

The model was applied to failure in high-porosity rocks. We analysed the yield curve of sandstones, and determined the values of the kinetic coefficients in the equation of damage evolution (35b) for Berea sandstone. A significant advantage of our model is the ability to mimic the entire yield curve, positive and negative slopes, by a single formulation. In our model the transition from positive to negative values in the yield curve is determined by the competition between two thermodynamic forces (35): the force caused by damage change and the force caused by inelastic porosity change. For low effective pressures the force caused by damage change dominates (positive slope of the curve), whereas for high effective pressure the force caused by inelastic porosity change dominates (negative slope).

Localization/delocalization are also determined by the competition between the forces caused by the changes in damage and inelastic porosity. It was shown by Lyakhovsky *et al.* (1997a) that the thermodynamic force caused by damage change contributes to localization of the damage for $\xi > \xi_0$. Localization will occur only if the latter force dominates, and transition to non-localized cataclastic flow will occur if the force caused by inelastic porosity variation, dominates. Our model reproduces experimental observations on the modes of failure in sandstones (Menendez *et al.* 1996; Wong *et al.* 1997; Baud *et al.* 2000), predicting the appearance of three modes of failure: cataclastic flow, compacting shear bands and dilating shear bands.

Our model also displays the experimentally observed connection between fluid pressure and deviatoric stresses. Moreover, the model highlights the role of damage evolution in the variation of fluid pressure. Under undrained conditions, fluid pressure varies due to two terms depending on mean stress and shear stress (eq. 1). Rising mean stress increases fluid pressure (according to Skempton coefficient B) and rising shear stress (at constant mean stress) decreases fluid pressure. In triaxial compression tests, where increasing the differential stress increases both the mean stress and the shear stress, fluid pressure first increases and then decreases, after the onset of damage. Our predictions on fluid pressure were found to be in quantitative agreement with undrained experiments on sandstones with constant damage (Fig. 5), as well as with kinetic processes when dilation was caused by microcracks (Fig. 7). The model explains dilatancy hardening observed in undrained experiments (Lockner & Stanchits 2002), suggesting that dilatancy hardening should be taken into consideration in predictions of Coulomb failure stress of faults.

The evolution of the porosity and the damage variable in our model resembles the evolution of the porosity and the state variable in some models of rate- and state-dependent friction (Sleep 1995; Segall & Rice 1995). In the latter models the evolution of the inelastic porosity is assumed to be analogous to the evolution of the frictional state variable. In our model, thermodynamic principles lead us to an antisymmetric matrix for the evolution of the inelastic porosity and the damage variable (eqs 30a and 30b), and therefore to a similar evolution for inelastic porosity and the damage variable. In addition, here like in Sleep's (1995) model, the evolution of the damage variable (or the state variable in Sleep 1995) is controlled by two terms: one related to ductile compaction and one to crack creation. These considerations indicate that there is a connection between our damage variable and the state variable, and that the similar evolution of the state variable and the inelastic porosity has a thermodynamic basis.

ACKNOWLEDGMENTS

The authors thank D. A. Lockner and Y. Ben-Zion for useful discussions, and two anonymous reviewers for their constructive comments on an earlier manuscript. YH and VL acknowledge support from the US-Israel Binational Science Foundation, grant BSF-9800198. AA thanks EU-INTAS for support (grant #01-0748).

REFERENCES

Agnon, A. & Lyakhovsky, V., 1995. Damage distribution and localization during dyke intrusion, in *The Physics and Chemistry of Dykes*, pp. 65–78, eds Baer, G. & Heimann A., Balkema, Rotterdam.

Aydin, A. & Johnson, A.M., 1978. Development of faults as zones of deformation bands and as slip surfaces in sandstone, *Pure appl. Geophys.*, **116,** 931–942.

Aydin, A. & Johnson, A.M., 1983. Analysis of faulting in porous sandstones, *J. Struct. Geol.*, **5,** 19–31.

Bart, M., Shao, J.F. & Lydzba, D., 2000. Poroelastic behavior of saturated brittle rock with anisotropic damage, *Int. J. Numer. Anal. Meth. Geomech.*, **24,** 1139–1154.

Baud, P., Zhu, W. & Wong, T.-f., 2000. Failure mode and weakening effect of water on sandstone, *J. geophys. Res.*, **105,** 16 371–16 389.

Bear, J., 1972. *Dynamics of Fluids in Porous Media*, American Elsevier, New York.

Bercovici, D., Ricard, Y. & Schubert, G., 2001. A two-phase model for compaction and damage, part 1: General Theory, *J. geophys. Res.*, **106,** 8887–8906.

Bernabe, Y. & Brace, W.F., 1990. Deformation and fracture of Berea sandstone, in *The Brittle-ductile Transition in Rocks, Geophys. Monogr.* **56,** pp. 91–101. eds Duba, A.G., Durham, W.B., Handin, J.W. & Wang, H.F., AGU, Washington DC.

Besuelle, P., 2001. Compacting and dilating shear bands in porous rock: theoretical and experimental conditions, *J. geophys. Res.*, **106,** 13 435–13 442.

Biot, M.A., 1941. General theory of three-dimensional consolidation, *J. appl. Phys.*, **12,** 155–164.

Biot, M.A., 1956. General solutions of the equations of elasticity and consolidation for a porous material, *J. appl. Mech.*, **78,** 91–96.

Biot, M.A., 1973. Nonlinear and semilinear rheology of porous solids, *J. geophys. Res.*, **78,** 4924–4937.

Biot, M.A. & Willis, D.G., 1957. The elastic coefficients of the theory of consolidation, *J. appl. Mech., Trans. ASME*, **79,** 596–601.

Birchwood, R.A. & Turcotte, D.L., 1994. A unified approach to geopressuring, low-permeability zone formation, and secondary porosity generation in sedimentary basins, *J. geophys. Res.*, **99,** 20 051–20 058.

Blanpied, M.L., Lockner, D.A. & Byerlee, J.D., 1992. An earthquake mechanism based on rapid sealing of faults, *Nature*, **358,** 574–576.

Byerlee, J.D., 1967. Frictional characteristics of granite under high confining pressure, *J. geophys. Res.*, **72,** 3639–3648.

Byerlee, J.D., 1990. Friction, overpressure and fault normal compression, *Geophys. Res. Lett.*, **17,** 2109–2112.

Byerlee, J., 1993. A model for episodic flow of high pressure water in fault zones before earthquakes, *Geology*, **21,** 303–306.

Christensen, R.M., 1979. *Mechanical of Composite Materials*, Wiley Inter-Science, New York.

Connolly, J.A.D. & Podladchikov, Y.Y., 2000. Temperature-dependent viscoelastic compaction and compartmentalization in sedimentary basins, *Tectonophysics*, **324,** 137–168.

Coussy, O., 1995. *Mechanics of Porous Continua*, Wiley, Chichester.

Dennis, S.M. & Atkinson, B.K., 1982. The influence of water on the stress supported by experimentally faulted Westerly granite, *Geophys. J. R. astr. Soc.*, **71,** 285–294.

Dieterich, J.H., 1979. Modeling of rock friction, 1, Experimental results and constitutive equations, *J. geophys. Res.*, **84,** 2161–2168.

Dieterich, J.H., 1981. Constitutive properties of faults with simulated gouge, in *Mechanical Behavior of Crustal Rocks: The Handin Volume, Geophys. Monogr. Ser.*, Vol. 24, pp. 103–120, AGU, Washington, DC.

Dvorkin, J. & Nur, A., 1996. Elasticity of high-porosity sandstones: theory for two North Sea data sets, *Geophysics*, **61,** 1363–1370.

Dvorkin, J., Nur, A. & Yin, H., 1994. Effective properties of cemented granular materials, *Mech. of Mater.*, **18,** 351–366.

Fitts, D.D., 1962. *Nonequilibrium Thermodynamics*, McGraw-Hill Book Company, New York.

Fowler, A.C., 1990. A compaction model for melt transport in the earth's asthenosphere. Part 1: the basic model, in *Magma Transport and Storage*, pp. 3–14, ed. Ryan, M.P., Wiley, New York.

Fowler, A.C. & Yang, X., 1999. Pressure solution and viscous compaction in sedimentary basins, *J. geophys. Res.*, **104,** 12 989–12 997.

Ge, S. & Stover, S.C., 2000. Hydrodynamic response to strike- and dip-slip faulting in a half-space, *J. geophys. Res.*, **105,** 25 513–25 524.

Gibbs, J.W., 1961. *The Scientific Papers*, *Thermodynamics*, **1,** Dover, New York.

deGroot, S.R. & Mazur, P., 1962. *Nonequilibrium Thermodynamics*, North-Holland Publishing Co., Amsterdam.

Hamiel, Y. et al., 2004, *Geophys. J. Int.*, submitted.

Hankel, D.J. & Wade, N.H., 1966. Plane strain tests on a saturated remolded clay, *J. Soil Mech. Found. Div. Am. Soc. Civ. Eng.*, **92,** 67–80.

Hansen, N.R. & Schreyer, H.L., 1994. A thermodynamically consistent framework for theories of elastoplasticity coupled with damage, *Int. J. Solids Structures*, **31,** 359–389.

Hickman, S., Sibson, R.H. & Bruhn, R., 1995. Introduco special section, mechanical involvement of fluids in faulting, *J. geophys. Res.*, **100,** 12 831–12 840.

Hoff, N.J., 1953. The necking and rupture of rods subjected to constant tensile loads, *J. appl. Mech.*, **20,** 105–108.

Hudson, J.A., 2000. The effect of fluid pressure on wave speeds in a cracked solid, *Geophys. J. Int.*, **143,** 302–310.

Issen, K.A. & Rudnicki, J.W., 2000. Conditions for compaction bands in porous rock, *J. geophys. Res.*, **105,** 21 529–21 536.

Ju, J.W., 1990. Isotropic and anisotropic damage variables in continuum damage mechanics, *J. Eng. Mech.*, **116,** 2764–2770.

Kachanov, L.M., 1958. On the time to rupture under creep conditions, *Izv. Acad. Nauk SSSR, OTN*, **8,** 26–31(in Russian).

Kachanov, L.M., 1986. *Introduction to Continuum Damage Mechanics*, pp. 135, Martinus Nijhoff Publishers, Dordrecht, the Netherlands.

Kachanov, M., 1994. On the concept of damage in creep and in the brittle-elastic range, *Int. J. Damage Mech.*, **3,** 329–337,

Lahner, F.K., 1995. A model for intergranular pressure solution in open systems, *Tectonophysics*, **245,** 153–170.

Liu, Y., Lyakhovsky, V., Ben-Zion, Y. & Lockner, D.A, 2001. Visco-elastic damage rheology model: theory and experimental verification. *In: EOS, Trans. AGU, 82(47), Fall Meet. Suppl.*, abstract T51A–0844.

Lockner, D.A. & Stanchits, S.A., 2002. Undrained poroelastic response of sandstones to deviatoric stress change, *J. geophys. Res.*, **107,** (B12), 2553, doi: 10.1029/2001JB001460.

Lockner, D.A., Byerlee, J.D., Kuksenko, V., Ponomarev, A. & Sidorin A., 1992. Observations of quasistatic fault growth from acoustic emissions, in *Fault Mechanics and Transport Properties of Rocks, International Geophysics Series*, Vol. 51, pp. 3–31, eds Evans, B. & Wong, T.-f., Academic Press, San Diego, CA.

Lyakhovsky, V.A. & Myasnikov, V.P., 1985. On the behavior of visco-elastic cracked solid, *Physics of Solid Earth*, **4,** 28–35.

Lyakhovsky, V., Ben-Zion, Y. & Agnon, A., 1997a. Distributed damage, faulting, and friction, *J. geophys. Res.*, **102,** 27 635–27 649.

Lyakhovsky, V., Reches, Z., Weinberger, R. & Scott, T.E., 1997b. Nonlinear elastic behavior of damaged rocks, *Geophys. J. Int.*, **130,** 157–166.

Malvern, L.E., 1969. *Introduction to the Mechanics of a Continuum Medium*, Prentice-Hall, Inc., Englewood Cliffs, New Jersey.

Masuda, K., 2001. Effects of water on rock strength in a brittle regime, *J. Struct. Geol.*, **23,** 1653–1657.

Mavko, G. & Mukerji, T., 1995. Seismic pore space compressibility and Gassmann's relation, *Geophysics*, **60,** 1743–1749.

McKenzie, D.P., 1984. The generation and compaction of partially molten rock, *J. Petrol.*, **25,** 713–765.

Menendez, B., Zhu, W. & Wong, T.-f., 1996. Micromechanics of brittle faulting and cataclstic flow in Berea sandstone, *J. Struct. Geol.*, **18,** 1–16.

Miller, S.A., Nur, A. & Olgaard, D.L., 1996. Earthquakes as acoupled shear stress- high pore pressure dynamical system, *Geophys. Res. Lett.*, **23,** 197–200.

Nikolaevsky, V.N., Vasniev, K.S., Gorbunov, A.T. & Zotov, G.A., 1970. *Mechanics of Saturated Porous Media*, Nedra, Moscow (in Russian).

Nur, A. & Byerlee, J.D., 1971. An exact effective stress law for elastic deformation of rock with fluids, *J. geophys. Res.*, **76,** 6414–6419.

Olsson, W.A., 1999. Theoretical and experimental investigation of compaction bands in porous rock, *J. geophys. Res.*, **104,** 7219–7228.

Onsager, L., 1931. Reciprocal relations in irreversible processes., *Phys. Rev.*, **37,** 405–416.

Paterson, M.S., 1978. *Experimental Rock Deformation—the Brittle Field*, Springer-Verlag, Berlin.

Paterson, M.S., 1995. A theory for granular flow accommodated by material transfer via an intergranular fluid, *Tectonophysics*, **245,** 135–151.

Poirier, J.-P., 1985. *Creep of Crystals*, Cambridge University Press, Cambridge.

Prigogine, I., 1955. *Introduction to Thermodynamics of Irreversible Processes*, Springfield, Illinois.

Rabotnov, Y.N., 1969. A mechanism of a long time failure, in *Creep Problems in Structural Members*, p. 822, ed. Leckie, F.A., North-Holland, Amsterdam.

Rabotnov, Y.N., 1988. *Mechanics of Deformable Solids*, p. 712, Science, Moscow.

Renshaw, C.E., 1995. On the relationship between mechanical and hydraulic apertures in rough-walled fractures, *J. geophys. Res.*, **100,** 24 629–24 636.

Renshaw, C.E., 1996. Influence of subcritical fracture growth on the connectivity of fracture networks, *Water Resour. Res.*, **32,** 1519–1530.

Rice, J.R., 1992. Fault stress states, pore pressure distribution, and the weakness of the San Andreas fault, in *Fault Mechanics and Transport Properties of Rocks*, pp. 476–503, eds Evans, B. & Wong T.-f., Academic Press, San Diego, CA.

Rice, J.R. & Cleary, M.P., 1976. Some basic stress diffusion solution for fluid-saturated elastic porous media with compressible constituents, *Rev. Geophy. Space Phys.*, **14,** 227–241.

Robinson, E.L., 1952. Effect of temperature variation on the long-term rupture strength of steels, *Trans. Am. Soc. Mech. Eng.*, **174,** 777–781.

Ruina, A., 1983. Slip instability and state variable friction laws, *J. geophys. Res.*, **88,** 10 359–10 370.

Rutter, E.H., 1983. Pressure solution in nature, theory and experiment, *J. geol. Soc. Lond.*, **140,** 725–740.

Sedov, L.I., 1968. Variational methods of constructing models of continuos media, in *Irreversible Aspects of Continuum Mechanics*, pp. 17–40, eds, Parkus, H. & Sedov, L.I., Springer-Verlag, New-York.

Segall, P. & Rice, J.R., 1995. Dilatancy, compaction, and slip instability of a fluid-infiltrated fault, *J. geophys. Res.*, **100,** 22 155–22 171.

Shao, J.F., 1998. Poroelastic behavior of brittle rock materials with anisotropic damage, *Mech. Mater.*, **30,** 41–53.

Skempton, A.W., 1954. The pore-pressure coefficients A and B, *Geotechnique*, **4,** 143–147.

Sleep, N.H., 1995. Ductile creep, compaction, and rate and state dependent friction within major fault zones, *J. geophys. Res.*, **100,** 13 065–13 080.

Sleep, N.H. & Blanpied, M.L., 1992. Creep, compaction and the weak rheology of major faults, *Nature*, **359,** 687–692.

Suetnova, E. & Vasseur, G., 2000. 1-D modeling rock compaction in sedimentary basins using a visco-elastic rheology, *Earth planet. Sci. Lett.*, **178,** 373–383.

Terzaghi, K., 1925. *Erdbaumechanik auf bodenphysikalischer grundlage*, Deuticke, Leipzig.

Valanis, K.C., 1990. A theory of damage in brittle materials, *Eng. Fract. Mech.*, **36,** 403–416.

Wong, T.-f. & Zhu, W., 1999. Brittle faulting and permeability evolution: Hydromechanical measurement, microstructural observation, and network modeling, in *Faults and Subsurface Fluid Flow in the Shallow crust, Geophys. Monogr* Vol. 113, 83–99, eds Haneberg, W.C., Mozley, P.S., Moore, J.C. & Goodwin, L.B., AGU, Washington DC.

Wong, T.-f., David, C. & Zhu, W., 1997. The transition from brittle faulting to cataclastic flow in porous sandstones: mechanical deformation, *J. geophys. Res.*, **102,** 3009–3025.

Yang, X.-S., 2001. A unified approach to mechanical compaction, pressure solution, mineral reactions and the temperature distribution in hydrocarbon basins, *Tectonophysics*, **330,** 141–151.

Zhang, J., Wong, T.-f. & Davies, D.M., 1990. Micromechanics of pressure-induced grain crushing in porous rocks, *J. geophys. Res.*, **95,** 341–352.

Zhu, W. & Wong, T.-f., 1996. Permeability reduction in a dilating rock: Network modeling of damage and tortuosity, *Geophys. Res. Lett.*, **23,** 3099–3102.

Zhu, W. & Wong, T.-f., 1997. The transition from brittle faulting to cataclastic flow: Permeability evolution, *J. geophys. Res.*, **102,** 3027–3041.